JACS
JOURNAL OF THE AMERICAN CHEMICAL SOCIETY
pubs.acs.org/JACS
Article

Prediction of Above-Room-Temperature Superconductivity in Lanthanide/Actinide Extreme Superhydrides

Xin Zhong,[#] Ying Sun,[#] Toshiaki Iitaka, Meiling Xu, Hanyu Liu,* Russell J. Hemley, Changfeng Chen,* and Yanming Ma*

Cite This: *J. Am. Chem. Soc.* 2022, 144, 13394−13400

ABSTRACT: Achieving room-temperature superconductivity has been an enduring scientific pursuit driven by broad fundamental interest and enticing potential applications. The recent discovery of high-pressure clathrate superhydride LaH_{10} with superconducting critical temperatures (T_c) of 250−260 K made it tantalizingly close to realizing this long-sought goal. Here, we report a remarkable finding based on an advanced crystal structure search method of a new class of extremely hydrogen-rich clathrate superhydride MH_{18} (M: rare-earth/actinide atom) stoichiometric compounds stabilized at an experimentally accessible pressure of 350 GPa. These compounds are predicted to host T_c up to 330 K, which is well above room temperature. The bonding and electronic properties of these MH_{18} clathrate superhydrides closely resemble those of atomic metallic hydrogen, giving rise to the highest T_c hitherto found in a thermodynamically stable hydride compound. An in-depth study of these extreme superhydrides offers insights for elucidating phonon-mediated superconductivity above room temperature in hydrogen-rich and other low-Z materials.

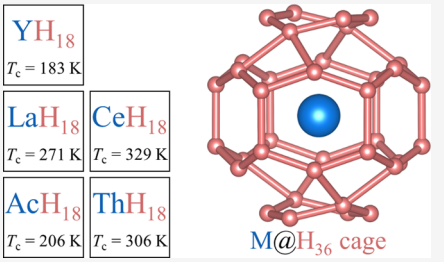

INTRODUCTION

The search for room-temperature superconductivity has been a long-standing scientific endeavor ever since Heike Kamerlingh Onnes discovered in 1911 that mercury could conduct electricity without resistance below a critical temperature around 4 K. Twenty-four years after the discovery of this phenomenon known as superconductivity, Wigner and Huntington[1] proposed that molecular hydrogen could undergo a phase transition into an atomic metallic hydrogen (AMH) phase at high pressures, which attracted great interest, especially after the conjecture of its ability to host very high-temperature superconductivity.[2−5] Creating AMH, however, has proven extremely challenging due to the stringent synthesis and characterization conditions at very high pressures, currently recognized to be above 500 GPa.[6−8] An early study found that hydrogen-rich metal hydride Th_4H_{15} was superconducting with a critical temperature T_c of 8 K at ambient pressure;[9] later studies found that chemical substitution or doping could stabilize hydrogen-containing compounds that may host metallic and superconducting states approaching that of AMH.[10,11] This line of work has been actively pursued after the conceptual development of using chemical precompression to facilitate the formation of hydrogen-dominant metallic alloys[12] that host phonon-mediated high-temperature superconductivity.

Recent years have witnessed concerted efforts of exploring routes to achieving high-T_c superconductivity in pressure-stabilized metal hydrides (*e.g.*, refs 13−16). Following the theoretical predictions of stabilizing H_2S[17] and H_3S[18] at high pressures, a high T_c of 203 K at 150 GPa was documented experimentally.[19] A different class of binary high-T_c metal (M) hydrides based on clathrate structure having stoichiometry MH_6[13−16,20−23] was predicted, led by the theoretical prediction on CaH_6.[23] Further efforts to reach higher T_c led to the prediction and discovery of superhydrides with stoichiometries MH_n with $n > 6$.[21,22,24] These efforts culminated in the experimental realization of superconducting LaH_{10} with a T_c of 250−260 K at pressures of 170−190 GPa,[25,26] followed by YH_9 with a T_c of 243 K at 201 GPa[27] and YH_6 with a T_c of 220 K at 166 or 237 GPa.[27,28] Very recently, the long-missing clathrate structured CaH_6 predicted in 2012 was successfully synthesized in the laboratory with a measured T_c of 215 K at 170 GPa.[29,30] Other notable cases of clathrate structured high-T_c hydrides include YH_{10},[21,22] Li_2MgH_{16},[31] and $CaYH_{12}$[32,33] from theory, and ThH_9 and ThH_{10}[34] from experiment. A recent work claimed possible room-temperature superconductivity in the C−S−H system,[35] but the structure and stoichiometry of the synthesized material remain unclear and require further investigation. An overriding idea underlying all of these efforts is to raise the hydrogen content while at the same time ensuring that the combination of compression and

Received: June 2, 2022
Published: July 12, 2022

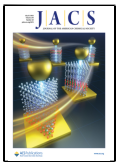

https://doi.org/10.1021/jacs.2c05834
J. Am. Chem. Soc. 2022, 144, 13394−13400

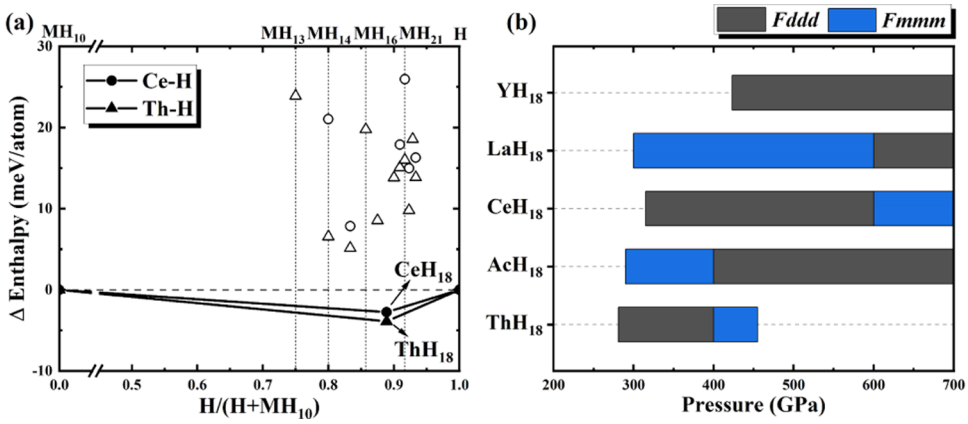

Figure 1. Calculated stability of predicted extreme superhydrides. (a) Calculated convex hull of newly identified extreme superhydrides CeH_{18} and ThH_{18}, both in the *Fddd* structure, calculated with respect to decomposition into Ce/ThH_{10}[22,34] and H_2[5] at 400 GPa. Data points located on the convex hull (solid lines) represent species stable against possible decomposition. The open symbols correspond to metastable/unstable compositions identified by the search process. (b) Stable pressure ranges of the predicted extreme superhydrides MH_{18} with respect to decomposition into known MH_x (x = 2, 4, 6, 9, 10, 12, 16, and 17) and *Cmca*−structured H_2; zero-point energy (ZPE) was included in the calculations.

chemical interactions are favorable to promote the H_2 molecules in the dense structure to create material configurations closely resembling AMH in bonding environments. In this regard, a major task has thus been to find superhydrides with proper electron-rich heavy atoms that are capable of stabilizing hydrogen in a nonmolecular form to generate T_c exceeding that of the established superhydrides such as LaH_{10}.[13,31,36,37]

Recent studies[15,16,21,22,34] showed that rare-earth (RE) and actinide (An) elements are capable of maintaining significant hydrogen by forming high-pressure clathrate compounds with a very high T_c. These results raise the exciting prospects of finding RE/An superhydrides containing even higher hydrogen content and hence further increased T_c that may approach or even exceed room temperature. Based on these considerations, we have explored electron-rich rare-earth and actinide elements that provide electrons to dissociate molecular hydrogen, thereby creating an AMH-like environment conducive to harboring high-T_c superconductivity. Using our developed structural search algorithms,[38,39] we uncovered a new class of hydrogen-superrich compounds with stoichiometry MH_{18} (M = RE or An atom). These extreme superhydrides exhibit unique H_{36} clathrate atomic cages with bonding environments similar to that predicted for AMH. First-principles calculations for different MH_{18} superhydrides predict diverse T_c values among the same stoichiometry that offer insights into the effect and nature of chemical precompression. Notable among these extreme superhydrides are CeH_{18} and ThH_{18} that exhibit above-room-temperature T_c near 330 K at 350 GPa and 321 K at 600 GPa, respectively, which represent the highest T_c values among all hitherto known thermodynamically stable superhydrides. The results of this study provide a wealth of information on material behaviors and key physics and chemistry insights that allow an in-depth study of the factors with major influence on achieving ultrahigh-temperature phonon-mediated superconductivity in hydrides, thereby opening a path for creating binary and multinary high-T_c superhydrides that can operate at or even above room temperature.

RESULTS AND DISCUSSION

We performed structure searches in binary hydrides MH_m (m = 2−24) over a wide range of hydrogen contents to predict stable structures, with a sharp focus on hydrogen-superrich phases. Particularly noteworthy was the finding of new stoichiometric Ce and Th extreme superhydrides Ce/ThH_{18} stable at experimentally accessible pressures[8,40] around 300 GPa after the zero-point energy (ZPE) was considered. Specifically, CeH_{18} and ThH_{18} become stable at reduced pressures of 315 and 281 GPa, respectively (see Figure 1a,b as well as Figure S1), making the experimental synthesis and characterization feasible. It is noted that these newly predicted extreme superhydrides possess higher T_c with competing synthesis pressure compared to the previously proposed high-T_c binary superhydride YH_{10}, which was not successfully synthesized in a recent experiment.[27] A recent work reported that materials synthesis could be achieved near terapascal pressures,[40] making it feasible to realize the materials predicted in this work. Further calculations for a broad range of RE and An hydride compounds up to 700 GPa reveal ubiquitous stability of the MH_{18} stoichiometry among diverse RE and An hydrides for RE/An = Y, La, Ce, Ac, and Th (Figure 1b and Tables S1 and S2). Details of the computational methods for the structure search and property calculations are provided in the Supporting Information.

Conspicuous in the predicted crystal structure of the MH_{18} extreme superhydrides is the H_{36} clathrate cage, which contrasts with the H_{24}, H_{29}, and H_{32} structural units found in previously identified hydrides with lower hydrogen contents. The peculiar three-dimensional hydrogen clathrate structure crystallizes in a unit cell with space group *Fddd* (Figure 2a) in which H_{36} cages are linked by a $6H_6$ ribbon-ring structure with two wrinkled H_6 hexagons above and below with bridge bonds connecting the H_6 hexagons to the $6H_6$ ribbon ring (Figure 2b,c). At higher pressures, depending on the choice of the M atom, the H_{36} clathrate units rearrange and stabilize in another structure with space group *Fmmm* (Figure 2b). Below we focus our analysis mainly on CeH_{18} to showcase its prominent properties while also discussing key data and trends involving other MH_{18} compounds.

https://doi.org/10.1021/jacs.2c05834
J. Am. Chem. Soc. 2022, 144, 13394−13400

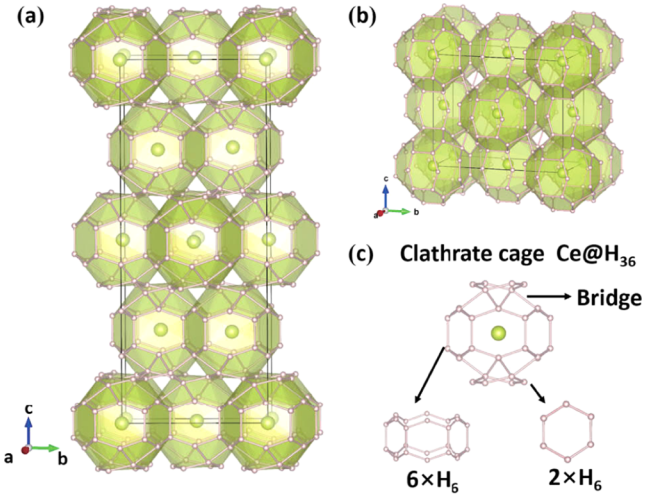

Figure 2. Crystal structure of MH_{18}. (a) *Fddd* and (b) *Fmmm* phase. (c) Building units of the $M@H_{36}$ hydrogen clathrate cage, including a $6H_6$ ribbon ring and two H_6 hexagons, which are connected by pertinent bridge bonding networks. The large and small spheres represent the metal and hydrogen atoms, respectively.

We first examine the high-pressure electronic structure of CeH_{18}. The results clearly indicate the CeH_{18} phase is metallic with several bands crossing the Fermi level (Figure 3a, left), and hydrogen atoms make a substantial contribution to the electronic density of states (DOS) near the Fermi level, which is almost identical to the DOS contributed by the electrons from Ce (Figure 3a, right). The DOS is essentially flat around the Fermi energy, which is notably different from the DOS of LaH_{10}, which exhibits a van Hove singularity near the Fermi energy.[21] The calculated band structures at different pressures reveal changes in band filling; notably, the hole-bands at the *X*-point, along the *Z*−*X* path, and at the *Y*-point move down with increasing pressure (see Figure S2), indicating a systematic pressure-driven electron transfer that suppresses T_c on further compression.

Turning to the phonons and electron−phonon coupling in CeH_{18}, the calculated phonon dispersion results are shown in Figure 3b, left. No imaginary phonon modes are present in the entire Brillouin zone, indicating the dynamic stability of this crystal structure. We then computed the Eliashberg spectral function $\alpha^2F(\omega)$, from which the electron−phonon coupling parameter can be obtained *via* a simple integration in the frequency domain. The resulting integrated electron−phonon coupling parameter $\lambda = 2.3$ is quite large and comparable to that found for H_3S ($\lambda = 2.2$).[18] Such strong electron−phonon coupling makes various approximate weak-coupling T_c formulas generally unreliable, and an accurate description necessitates direct numerical solutions to the Eliashberg equations.[41,42] Adopting the latter method, we calculated superconducting energy gap and transition temperature and varied the Coulomb pseudopotential from $\mu^* = 0.10$ (as is typically used) to $\mu^* = 0.13$ to estimate a reasonable range of T_c values. The resulting T_c of 309−329 K (for $\mu^* = 0.10$ and 0.13) at 350 GPa, where CeH_{18} is stable, is well above the room temperature. These results are significantly higher than the highest T_c predicted for previously reported Ce superhydrides with lower hydrogen contents (*e.g.*, $T_c = 117$ K for CeH_9)[43] and represent the highest predicted T_c among all known thermodynamically stable superhydrides.[22]

To elucidate the underlying mechanisms for the predicted superconductivity of these extreme superhydrides, we calculated electronic, phonon, and electron−phonon coupling parameters, and the resulting critical temperatures using the Eliashberg equations of other selected MH_{18} compounds. We also performed identical calculations for pure AMH in the $I4_1/amd$ structure, which is predicted to be stable or metastable in the same pressure range.[44] First, we note that systematic examination of the energetics and dynamic stability of the MH_{18} structures beyond their stability fields reveal metastability to lower pressures of phases that maintain high superconducting temperatures (Figure 1b). The pressure dependence of T_c for the identified stable and metastable phases of MH_{18} and $I4_1/amd$ hydrogen is given in Figure 4. The T_c values are distributed over a large range, from 50 K for *Fddd*-AcH_{18} at 700 GPa up to near 330 K for *Fddd*-CeH_{18} at 350 GPa ($\mu^* = 0.10$). Moreover, the resulting critical temperatures vary considerably among the MH_{18} superhydrides at the same pressure. The associated microscopic properties of each phase listed in Table 1 detail the differences in superconducting behavior among the compounds. The disparities within the same stoichiometry and clathrate structures stem from their characteristic vibrational frequencies, electron−phonon coupling parameters λ, and electronic DOS at the Fermi level $N(E_f)$. We also have calculated the charge transfer for CeH_{18} and LaH_{18}, and the results (Table S1) show charge transfer from metal Ce/La to hydrogen atoms. The T_c values for different MH_{18} structures may also be related to the different *f* electron fillings, *e.g.*, there are different T_c values for different MH_{10} superhydrides as previously reported.[22]

The present findings offer important clues for understanding the trends in superhydride T_c values that approach that of AMH at high pressures. Among the extreme superhydrides, CeH_{18} exhibits the highest T_c over the entire pressure range, with nearest-neighbor H−H distances of 0.85−1.17 Å, close to that of $I4_1/amd$ structured AMH (1.0 Å) at 500 GPa. The calculated projected phonon DOS from the Ce and H atoms (Figure 3b) shows that the main contributions to the EPC come from the mid- and high-frequency hydrogen vibrations at 500−2500 cm^{-1}. Further, most of MH_{18} compounds exhibit monotonically decreasing T_c with increasing pressure, the exception being both *Fddd*- and *Fmmm*-ThH_{18} for which T_c slightly increases on compression. The decrease in T_c with pressure of most superhydrides[21,22] is reminiscent of the behavior of AMH at higher pressures (700−1,000 GPa),[5] which is consistent with the idea that chemical precompression in hydrogen compounds shifts their material behavior toward lower pressures. These insights are helpful for continued exploration and rational design of optimal superconducting superhydrides.

We consider additional effects such as spin−orbit coupling (SOC), magnetism, and electron correlation that may affect the estimated T_c of the predicted MH_{18} compounds. We take the highest T_c extreme superhydrides CeH_{18} and ThH_{18} as examples to assess these effects. Our calculations reveal that the T_c values are insensitive to SOC (Table 1), which is consistent with the nearly identical band structures calculated with and without the SOC (Figure 3a). We examined the energetics of the magnetic structures of the predicted MH_{18} compounds by considering six possible magnetic configurations (one ferromagnetic and five antiferromagnetic configurations). The results show that the nonmagnetic state is the

https://doi.org/10.1021/jacs.2c05834
J. Am. Chem. Soc. 2022, 144, 13394−13400

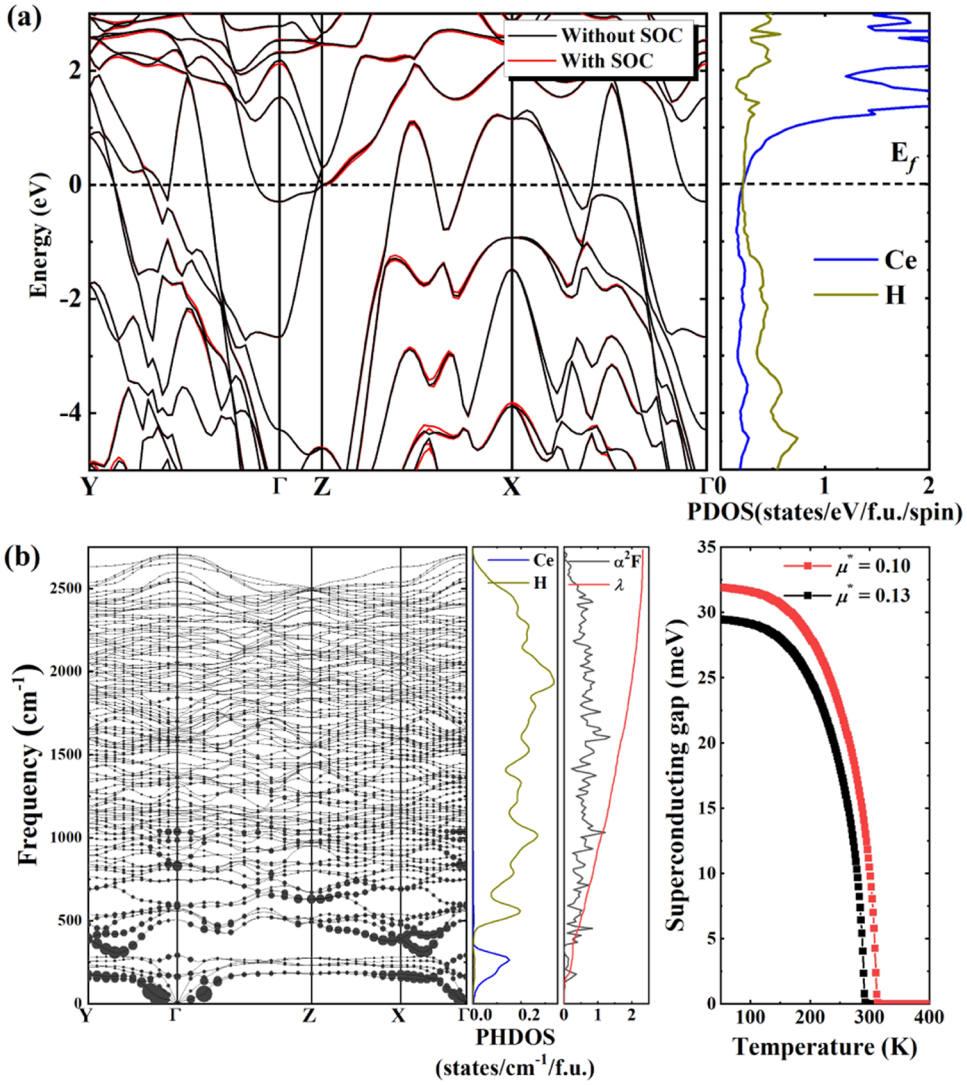

Figure 3. Electronic structures of CeH_{18}. (a) Electronic band structure (left) and projected density of states (right) of CeH_{18} at 400 GPa. The band structures without and with the inclusion of SOC are plotted with black and red lines, respectively. (b) Phonon dispersion curves with the strength of q resolved λ_q indicated by circle size (left), phonon density of states (PHDOS), Eliashberg spectral function $\alpha^2F(\omega)$ and EPC parameter $\lambda(\omega)$ (middle), and superconducting energy gap (right) of CeH_{18} at 400 GPa.

most stable among all of the predicted MH_{18} compounds. A recent work quantified the correlation between the f orbital states at the Fermi energy with T_c for the lanthanide hydrides.[45] These results offer insights into the reason for CeH_{18} and ThH_{18} hosting high T_c values due to the fact that both Ce and Th elements have less partially filled f electron states. Although we have not considered electron correlation effects on the EPC due to a lack of available computational tools, we note that previous studies[18,21−23] have shown that the experimental results on several hydrides and superhydrides (*e.g.*, those of La, Y, Th, and Ca[25−30,34,46]) are well described by the theoretical results obtained within the current EPC computation scheme without considering the electron correlation effects. On this basis, it is expected that the results in the present work offer a reasonably accurate description of the superconductivity in the newly predicted MH_{18} compounds. For other RE/An hydrides that are not discussed in this work, especially those with more filled f electron states, it is expected that the magnetic, SOC, and strong correlation effects play more prominent roles, and other hydrogen-rich superconducting hydrides cannot be ruled out. However, phonon-mediated superconductivity is unlikely to be the underlying mechanism in these systems, and related studies are beyond the scope of this work.

CONCLUSIONS

Extreme superhydrides represent a class of hydrogen-rich materials containing the highest atomic hydrogen content among binary metal hydrides reported to date. The structures of these MH_{18} compounds consist of unique H_{36} clathrate units stabilized under pressure starting around 300−400 GPa. Superconducting critical temperatures exceeding room temperature arise from favorable electronic density of states near the Fermi level and the large phonon energy scale of the vibration modes, as well as the strong electron−phonon coupling, as demonstrated for CeH_{18} and ThH_{18}. Meanwhile, other MH_{18} compounds exhibit a wide range of T_c with variable combinations of electronic, phonon, and electron−phonon coupling. Recent focus in this research field has been mostly on reaching higher critical temperatures in ternary and higher

https://doi.org/10.1021/jacs.2c05834
J. Am. Chem. Soc. 2022, 144, 13394−13400

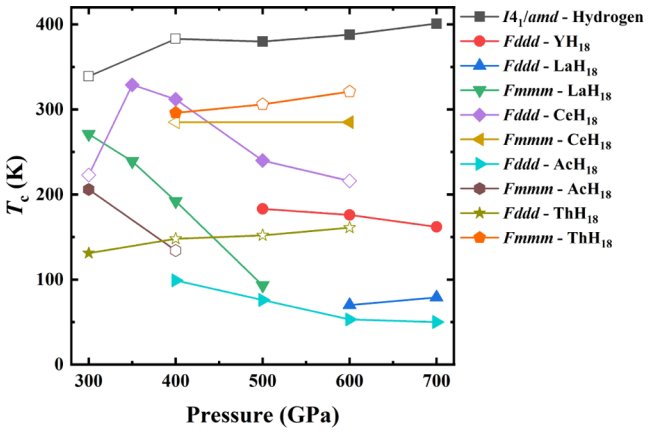

Figure 4. Superconducting critical temperatures of the predicted extreme superhydrides. Calculated T_c ($\mu^* = 0.10$) for selected extreme superhydrides MH_{18} compared with the results for the $I4_1/amd$ phase of solid hydrogen at high pressures. Solid (open) symbols represent the T_c data for stable (metastable) structural phases of the indicated MH_{18} compounds and atomic metallic hydrogen.

Table 1. Superconductivity of Predicted Structures[a]

compound	P	λ	ω_{log}	$N(E_f)$	T_c	T_c(SOC)
H-$I4_1/amd$	300	2.34	1577	0.23	339(320)	
H-$I4_1/amd$	400	2.39	1719	0.25	383(362)	
H-$I4_1/amd$	500	2.24	1806	0.23	380(356)	
H-$I4_1/amd$	600	2.10	1953	0.23	388(362)	
H-$I4_1/amd$	700	2.08	2021	0.25	401(375)	
YH_{18}-*Fddd*	500	1.50	1082	0.22	183(165)	
YH_{18}-*Fddd*	600	1.28	1467	0.21	176(158)	
YH_{18}-*Fddd*	700	1.10	1704	0.20	162(140)	
LaH_{18}-*Fddd*	600	0.74	1638	0.16	70(55)	
LaH_{18}-*Fddd*	700	0.78	1642	0.17	79(64)	
LaH_{18}-*Fmmm*	300	2.46	1156	0.25	271(255)	
LaH_{18}-*Fmmm*	350	1.68	1491	0.23	239(222)	
LaH_{18}-*Fmmm*	400	1.28	1649	0.22	192(174)	
LaH_{18}-*Fmmm*	500	0.82	1663	0.17	93(76)	
CeH_{18}-*Fddd*	300	2.03	985	0.27	223(207)	224(208)
CeH_{18}-*Fddd*	350	2.80	919	0.32	329(309)	330(310)
CeH_{18}-*Fddd*	400	2.32	1294	0.33	312(292)	310(290)
CeH_{18}-*Fddd*	500	1.85	920	0.27	240(212)	
CeH_{18}-*Fddd*	600	1.64	844	0.26	216(194)	
CeH_{18}-*Fmmm*	400	2.21	1260	0.22	285(265)	
CeH_{18}-*Fmmm*	600	1.76	1388	0.22	285(262)	
AcH_{18}-*Fddd*	400	0.92	1411	0.18	99(83)	
AcH_{18}-*Fddd*	500	0.80	1480	0.17	76(62)	
AcH_{18}-*Fddd*	600	0.65	1718	0.17	53(40)	
AcH_{18}-*Fddd*	700	0.62	1844	0.18	50(37)	
AcH_{18}-*Fmmm*	300	1.68	1217	0.23	206(190)	
AcH_{18}-*Fmmm*	400	1.36	904	0.20	134(119)	
ThH_{18}-*Fddd*	300	1.15	1227	0.21	131(116)	
ThH_{18}-*Fmmm*	400	3.39	568	0.37	296(277)	296(277)
ThH_{18}-*Fmmm*	500	1.92	1573	0.40	306(284)	306(285)
ThH_{18}-*Fmmm*	600	2.13	1331	0.42	321(299)	321(299)

[a]Calculated pressure (P (GPa)) variation of λ, ω_{log} (K), N (E_f) (states/Ry/atom/spin) and T_c (K) for $\mu^* = 0.10(0.13)$ for selected MH_{18} compounds in *Fmmm* or *Fddd* phase and hydrogen in the $I4_1/amd$ structure.[5,44,55]

multinary hydrides; the present work raises remarkable prospects that the bonding and electronic properties of the newly identified extreme binary superhydrides parallel those of atomic metallic hydrogen, giving rise to the highest T_c values among all known thermodynamically stable superhydrides. Furthermore, we have examined the influence of various heavy elements in hydrogen-rich superconductors over a range of pressures, and the resulting insights extend and refine the original conjecture of reducing the pressure for achieving AMH-like superconductivity by chemical doping and chemical precompression. Additional considerations of electron-[31] or hole-[47]doping effects in these extreme superhydrides may provide a promising platform for further exploration and optimization of superconductors that may host extraordinary above-room-temperature superconductivity.

COMPUTATIONAL METHODS

Our structure search is based on the PSO algorithm[48,49] as implemented in the CALYPSO methodology.[38,39] In an attempt to investigate the stable and metastable structures of MH_x ($x = 2-24$; M stands for rare-earth/actinide metals), we have performed structure searches of MH_x at 400 GPa. We have first performed structure searches for the crystal structures of the ThH_x ($x = 2-24$) series at 400 GPa with simulation cells containing one to four formula units up to 50 atoms per cell. These structure searches found that ThH_{18} holds the highest atomic hydrogen content among all known/predicted hydrides reported to date, and its superconducting T_c is very high (the estimated T_c of ThH_{18}-*Fmmm* is in the range of 296−321 K in the pressure range of 400−600 GPa), which motivated us to focus on the MH_{18} chemical composition. The other structures of MH_x stoichiometry were established by substituting the elements into the known structures of ThH_x ($x = 2$, 4, 6, 9, 10, 12, 16, 17, and 18). Our searches found that MH_{18} (M = Sc, Pr, Nd, Pm, Sm, Eu, Gd, Tb, Dy, Ho, Er, Tm, Yb, Lu, Pa, U, Np, Pu, Am, Cm, and Cf) are unstable in the pressure range of 0−700 GPa. We then performed further variable-stoichiometry structure searches that are able to explore the most stable structure among a broad range of stoichiometries selected for the stable MH_x (M = Y, La, Ce, and Ac; $x = 2-24$) system at 400 GPa, and the results of these additional searches confirm the above-identified stability of MH_{18} (M = Y, La, Ce, Ac, and Th). Structural optimization and computations of enthalpy, phonon, electronic structures, and spin−orbit coupling (SOC) were all performed in the framework of density functional theory (DFT) as implemented in the VASP code.[50] The Perdew−Burke−Ernzerhof[51] generalized gradient approximation (GGA)[52] was employed, and a kinetic cutoff energy of 500 eV was adopted. The zero-point energy (ZPE) of predicted compounds was obtained from lattice dynamic calculations as implemented in the PHONOPY code.[53] The electron−phonon coupling calculations were carried out using the QUANTUM ESPRESSO code.[54] Ultrasoft pseudopotentials for RE/An and H elements were used with a kinetic energy cutoff of 80 Ry. To reliably calculate the electron−phonon coupling in these metallic systems, we employed k-meshes of $2\pi \times 0.045$ Å^{-1} for the electronic Brillouin zone integration and q-meshes of $2\pi \times 0.09$ Å^{-1} for all of the phonon calculations.

ASSOCIATED CONTENT

Supporting Information

The Supporting Information is available free of charge at https://pubs.acs.org/doi/10.1021/jacs.2c05834.

Computational details of the structure prediction and electron−phonon coupling simulations for predicted MH_{18} structures; stability; electronic structures; and detailed structure information of predicted MH_{18} structures (PDF)

Structure.zip (ZIP)

https://doi.org/10.1021/jacs.2c05834
J. Am. Chem. Soc. 2022, 144, 13394−13400

AUTHOR INFORMATION

Corresponding Authors

Hanyu Liu − *State Key Laboratory of Superhard Materials and International Center for Computational Method & Software, College of Physics, Jilin University, Changchun 130012, China; International Center of Future Science, Jilin University, Changchun 130012, China;* orcid.org/0000-0003-2394-5421; Email: lhy@calypso.cn

Changfeng Chen − *Department of Physics and Astronomy, University of Nevada, Las Vegas, Nevada 89154, United States*; Email: changfeng.chen@unlv.edu

Yanming Ma − *State Key Laboratory of Superhard Materials and International Center for Computational Method & Software, College of Physics, Jilin University, Changchun 130012, China; International Center of Future Science, Jilin University, Changchun 130012, China;* orcid.org/0000-0003-3711-0011; Email: mym@jlu.edu.cn

Authors

Xin Zhong − *State Key Laboratory of Superhard Materials and International Center for Computational Method & Software, College of Physics, Jilin University, Changchun 130012, China; Key Laboratory of Functional Materials Physics and Chemistry of the Ministry of Education, College of Physics, Jilin Normal University, Changchun 130103, China;* orcid.org/0000-0003-3327-1045

Ying Sun − *State Key Laboratory of Superhard Materials and International Center for Computational Method & Software, College of Physics, Jilin University, Changchun 130012, China*

Toshiaki Iitaka − *Discrete Event Simulation Research Team, RIKEN Center for Computational Science, Wako, Saitama 351-0198, Japan*

Meiling Xu − *Laboratory of Quantum Functional Materials Design and Application, School of Physics and Electronic Engineering, Jiangsu Normal University, Xuzhou 221116, China;* orcid.org/0000-0001-6592-8975

Russell J. Hemley − *Departments of Physics, Chemistry, and Earth and Environmental Sciences, University of Illinois Chicago, Chicago, Illinois 60607, United States;* orcid.org/0000-0001-7398-8521

Complete contact information is available at: https://pubs.acs.org/10.1021/jacs.2c05834

Author Contributions

#X.Z. and Y.S. equally contributed to this work. The manuscript was written through contributions of all authors. All authors have given approval to the final version of the manuscript.

Funding

This work was supported by the National Key Research and Development Program of China (grant no. 2021YFA1400203), the Major Program of the National Natural Science Foundation of China (grant no. 52090024), National Natural Science Foundation of China (grant no. 12074138), Jilin Province Science and Technology Development Program (grant no. YDZJ202102CXJD016), Program for Jilin University Science and Technology Innovative Research Team, the Program for Jilin University Computational Interdisciplinary Innovative Platform, the Strategic Priority Research Program of Chinese Academy of Sciences (grant no. XDB33000000), National Science Foundation (grant no. DMR-210488), and computing facilities at the High-Performance Computing Centre of Jilin University and computing facilities at HOKUSAI system in RIKEN (Japan). This work is dedicated to the 70th anniversary of the physics of Jilin University.

Notes

The authors declare no competing financial interest.

REFERENCES

(1) Wigner, E.; Huntington, H. B. On the possibility of a metallic modification of hydrogen. *J. Chem. Phys.* **1935**, *3*, 764−770.
(2) Ashcroft, N. W. Metallic hydrogen: a high-temperature superconductor? *Phys. Rev. Lett.* **1968**, *21*, 1748−1749.
(3) Zhang, L.; Niu, Y.; Li, Q.; et al. Ab initio prediction of superconductivity in molecular metallic hydrogen under high pressure. *Solid State Commun.* **2007**, *141*, 610−614.
(4) Cudazzo, P.; Profeta, G.; Sanna, A.; et al. Ab initio description of high-temperature superconductivity in dense molecular hydrogen. *Phys. Rev. Lett.* **2008**, *100*, No. 257001.
(5) McMahon, J. M.; Ceperley, D. M. High-temperature superconductivity in atomic metallic hydrogen. *Phys. Rev. B* **2011**, *84*, No. 144515.
(6) Dias, R. P.; Silvera, I. F. Observation of the Wigner-Huntington transition to metallic hydrogen. *Science* **2017**, *355*, 715−718.
(7) Eremets, M. I.; Drozdov, A. P.; Kong, P. P.; Wang, H. Semimetallic molecular hydrogen at pressure above 350 GPa. *Nat. Phys.* **2019**, *15*, 1246−1249.
(8) Loubeyre, P.; Occelli, F.; Dumas, P. Synchrotron infrared spectroscopic evidence of the probable transition to metal hydrogen. *Nature* **2020**, *577*, 631−635.
(9) Satterthwaite, C. B.; Toepke, I. L. Superconductivity of hydrides and deuterides of thorium. *Phys. Rev. Lett.* **1970**, *25*, 741−743.
(10) Gilman, J. J. Lithium dihydrogen fluoride-an approach to metallic hydrogen. *Phys. Rev. Lett.* **1971**, *26*, 546−548.
(11) Carlsson, A. E.; Ashcroft, N. W. Approaches for reducing the insulator-metal transition pressure in hydrogen. *Phys. Rev. Lett.* **1983**, *50*, 1305−1308.
(12) Ashcroft, N. W. Hydrogen dominant metallic alloys: high temperature superconductors? *Phys. Rev. Lett.* **2004**, *92*, No. 187002.
(13) Zhang, L.; Wang, Y.; Lv, J.; Ma, Y. Materials discovery at high pressures. *Nat. Rev. Mater.* **2017**, *2*, No. 17005.
(14) Wang, H.; Li, X.; Gao, G.; Li, Y.; Ma, Y. Hydrogen-rich superconductors at high pressures. *WIREs Comput. Mol. Sci.* **2018**, *8*, No. e1330.
(15) Flores-Livas, J. A.; Boeri, L.; Sanna, A.; et al. A perspective on conventional high-temperature superconductors at high pressure: Methods and materials. *Phys. Rep.* **2020**, *856*, 1−78.
(16) Lv, J.; Sun, Y.; Liu, H.; Ma, Y. Theory-orientated discovery of high-temperature superconductors in superhydrides stabilized under high pressure. *Matter Radiat. Extremes* **2020**, *5*, No. 068101.
(17) Li, Y.; Hao, J.; Liu, H.; Li, Y.; Ma, Y. The metallization and superconductivity of dense hydrogen sulfide. *J. Chem. Phys.* **2014**, *140*, No. 174712.
(18) Duan, D.; Liu, Y.; Tian, F.; et al. Pressure-induced metallization of dense $(H_2S)_2H_2$ with high-T_c superconductivity. *Sci. Rep.* **2015**, *4*, No. 6968.
(19) Drozdov, A. P.; Eremets, M. I.; Troyan, I. A.; Ksenofontov, V.; Shylin, S. I. Conventional superconductivity at 203 kelvin at high pressures in the sulfur hydride system. *Nature* **2015**, *525*, 73−76.
(20) Li, Y.; Hao, J.; Liu, H.; et al. Pressure-stabilized superconductive yttrium hydrides. *Sci. Rep.* **2015**, *5*, No. 9948.
(21) Liu, H.; Naumov, I. I.; Hoffmann, R.; Ashcroft, N. W.; Hemley, R. J. Potential high-T_c superconducting lanthanum and yttrium hydrides at high pressure. *Proc. Natl. Acad. Sci. U.S.A.* **2017**, *114*, 6990−6995.
(22) Peng, F.; Sun, Y.; Pickard, C. J.; et al. Hydrogen clathrate structures in rare earth hydrides at high pressures: Possible route to

room-temperature superconductivity. *Phys. Rev. Lett.* **2017**, *119*, No. 107001.
(23) Wang, H.; Tse, J. S.; Tanaka, K.; Iitaka, T.; Ma, Y. Superconductive sodalite-like clathrate calcium hydride at high pressures. *Proc. Natl. Acad. Sci. U.S.A.* **2012**, *109*, 6463−6466.
(24) Geballe, Z. M.; Liu, H.; Mishra, A. K.; et al. Synthesis and stability of lanthanum superhydrides. *Angew. Chem.* **2018**, *130*, 696−700.
(25) Somayazulu, M.; Ahart, M.; Mishra, A. K.; et al. Evidence for superconductivity above 260 K in lanthanum superhydride at megabar pressures. *Phys. Rev. Lett.* **2019**, *122*, No. 027001.
(26) Drozdov, A. P.; Kong, P. P.; Minkov, V. S.; et al. Superconductivity at 250 K in lanthanum hydride under high pressures. *Nature* **2019**, *569*, 528−531.
(27) Kong, P. P.; Minkov, V. S.; et al. Superconductivity up to 243 K in yttrium hydrides under high pressure. *Nat. Commun.* **2021**, *12*, No. 5075.
(28) Troyan, I. A.; Semenok, D. V.; Kvashnin, A. G.; et al. Anomalous high-temperature superconductivity in YH_6. *Adv. Mater.* **2021**, *33*, No. 2006832.
(29) Ma, L.; Wang, K.; et al. High-temperature superconducting phase in clathrate calcium hydride CaH_6 up to 215 K at a pressure of 172 GPa. *Phys. Rev. Lett.* **2022**, *128*, No. 167001.
(30) Li, Z. W.; He, X.; Zhang, C.; et al. Superconductivity above 200 K discovered in superhydrides of calcium. *Nat. Commun.* **2022**, *13*, No. 2863.
(31) Sun, Y.; Lv, J.; Xie, Y.; Liu, H.; Ma, Y. Route to a superconducting phase above room temperature in electron-doped hydride compounds under high pressure. *Phys. Rev. Lett.* **2019**, *123*, No. 097001.
(32) Liang, X.; Bergara, A.; Wang, L.; et al. Potential high-Tc superconductivity in $CaYH_{12}$ under pressure. *Phys. Rev. B* **2019**, *99*, No. 100505.
(33) Xie, H.; Duan, D.; Shao, Z.; et al. High-temperature superconductivity in ternary clathrate $YCaH_{12}$ under high pressures. *J. Phys.: Condens. Matter* **2019**, *31*, No. 245404.
(34) Semenok, D. V.; Kvashnin, A. G.; Ivanova, A. G.; et al. Superconductivity at 161 K in thorium hydride ThH_{10}: Synthesis and properties. *Mater. Today* **2020**, *33*, 36−44.
(35) Snider, E.; Dasenbrock-Gammon, N.; McBride, R.; et al. Room-temperature superconductivity in a carbonaceous sulfur hydride. *Nature* **2020**, *586*, 373−377.
(36) Kruglov, I. A.; Semenok, D. V.; Song, H.; et al. Superconductivity of LaH_{10} and LaH_{16} polyhydrides. *Phys. Rev. B* **2020**, *101*, No. 024508.
(37) Wang, X.; Li, M.; Zheng, F.; Zhang, P. Crystal structure prediction of uranium hydrides at high pressure: A new hydrogen-rich phase. *Phys. Lett. A* **2018**, *382*, 2959−2964.
(38) Wang, Y.; Lv, J.; Zhu, L.; Ma, Y. CALYPSO: A method for crystal structure prediction. *Comput. Phys. Commun.* **2012**, *183*, 2063−2070.
(39) Wang, Y.; Lv, J.; Zhu, L.; Ma, Y. Crystal structure prediction via particle-swarm optimization. *Phys. Rev. B* **2010**, *82*, No. 094116.
(40) Dubrovinsky, L.; Khandarkhaeva, S.; Fedotenko, T.; et al. Materials synthesis at terapascal static pressures. *Nature* **2022**, *605*, 274−278.
(41) Sanna, A.; Flores-Livas, J.; Davydov, A. A.; Profeta, G.; Dewhurst, K.; Sharma, S.; Gross, E. K. U. Ab initio eliashberg theory: Making genuine predictions of superconducting features. *J. Phys. Soc. Jpn.* **2018**, *87*, No. 041012.
(42) The elk code, http://elk.sourceforge.net/, accessed 2018-06-01.
(43) Salke, N. P.; Esfahani, M. M. D.; Zhang, Y.; et al. Synthesis of clathrate cerium superhydride CeH_9 at 80-100 GPa with atomic hydrogen sublattice. *Nat. Commun.* **2019**, *10*, No. 4453.
(44) McMahon, J. M.; Ceperley, D. M. Ground-state structures of atomic metallic hydrogen. *Phys. Rev. Lett.* **2011**, *106*, No. 165302.
(45) Sun, W.; Kuang, X.; Keen, H. D. J.; Lu, C.; Hermann, A. Second group of high-pressure high-temperature lanthanide polyhydride superconductors. *Phys. Rev. B* **2020**, *102*, No. 144524.
(46) Snider, E.; Dasenbrock-Gammon, N.; McBride, R.; et al. Synthesis of yttrium superhydride superconductor with a transition temperature up to 262 K by Catalytic hydrogenation at high pressures. *Phys. Rev. Lett.* **2021**, *126*, No. 117003.
(47) Ge, Y.; Zhang, F.; Hemley, R. J. Room-temperature superconductivity in boron- and nitrogen-doped lanthanum superhydride. *Phys. Rev. B* **2021**, *104*, No. 214505.
(48) Kennedy, J.; Eberhart, R. In *Particle Swarm Optimization*, Proceedings of ICNN'95 - International Conference on Neural Networks, 1995; pp 1942−1948.
(49) Eberhart, R.; Kennedy, J. In *A New Optimizer Using Particle Swarm Theory*, MHS'95. Proceedings of the Sixth International Symposium on Micro Machine and Human Science, 1995; pp 39−43.
(50) Kresse, G.; Furthmüller, J. Efficient iterative schemes for ab initio total-energy calculations using a plane-wave basis set. *Phys. Rev. B* **1996**, *54*, 11169−11186.
(51) Perdew, J. P.; Wang, Y. Accurate and simple analytic representation of the electron-gas correlation energy. *Phys. Rev. B* **1992**, *45*, 13244−13249.
(52) Perdew, J. P.; Burke, K.; Ernzerhof, M. Generalized gradient approximation made simple. *Phys. Rev. Lett.* **1996**, *77*, 3865−3868.
(53) Togo, A.; Oba, F.; Tanaka, I. First-principles calculations of the ferroelastic transition between rutile-type and $CaCl_2$-type SiO_2 at high pressures. *Phys. Rev. B* **2008**, *78*, No. 134106.
(54) Giannozzi, P.; Baroni, S.; Bonini, N.; et al. QUANTUM ESPRESSO: a modular and open-source software project for quantum simulations of materials. *J. Phys.: Condens. Matter* **2009**, *21*, No. 395502.
(55) Pickard, C. J.; Needs, R. J. Structure of phase III of solid hydrogen. *Nat. Phys.* **2007**, *3*, 473−476.

https://doi.org/10.1021/jacs.2c05834
J. Am. Chem. Soc. 2022, 144, 13394−13400